

# Development of Small Molecule Inhibitors and Probes of Human SUMO Deconjugating Proteases

Victoria E. Albrow,<sup>1</sup> Elizabeth L. Ponder,<sup>2</sup> Domenico Fasci,<sup>3</sup> Miklós Békés,<sup>3</sup> Edgar Deu,<sup>1</sup> Guy S. Salvesen,<sup>3</sup> and Matthew Bogyo<sup>1,2,\*</sup>

<sup>1</sup>Department of Pathology

<sup>2</sup>Department of Microbiology and Immunology

Stanford University School of Medicine, 300 Pasteur Drive, Stanford, CA 94305, USA

<sup>3</sup>Program in Apoptosis and Cell Death Research, Burnham Institute for Medical Research, 10901 North Torrey Pines Road, La Jolla, CA 92037, USA

\*Correspondence: [mbogyo@stanford.edu](mailto:mbogyo@stanford.edu)

DOI 10.1016/j.chembiol.2011.05.008

## SUMMARY

Sentrin specific proteases (SENPs) are responsible for activating and deconjugating SUMO (Small Ubiquitin-like MOdifier) from target proteins. It remains difficult to study this posttranslational modification due to the lack of reagents that can be used to block the removal of SUMO from substrates. Here, we describe the identification of small molecule SENP inhibitors and active site probes containing azaepoxide and acyloxymethyl ketone (AOMK) reactive groups. Both classes of compounds are effective inhibitors of hSENPs 1, 2, 5, and 7 while only the AOMKs efficiently inhibit hSEN6. Unlike previous reported peptide vinyl sulfones, these compounds covalently labeled the active site cysteine of multiple recombinantly expressed SENP proteases and the AOMK probe showed selective labeling of these SENPs when added to complex protein mixtures. The AOMK compounds therefore represent promising new reagents to study the process of SUMO deconjugation.

## INTRODUCTION

The small ubiquitin-like modifier (SUMO) is an 11 kDa protein that is conjugated to various target proteins in order to alter their function (for reviews, see Drag and Salvesen, 2008; Geiss-Friedlander and Melchior, 2007; Kim and Baek, 2009). SUMO, like the structurally related ubiquitin protein modifier, is attached to substrate proteins through an isopeptide linkage to a lysine residue. This posttranslational process is orchestrated by a series of conjugating enzymes that activate and transfer the SUMO to the target protein. Prior to entering into the conjugation pathway, SUMO must first be proteolytically processed from a pro-form by the action of a SUMO-specific protease (SENP). SENP proteases also remove SUMO from a target to complete the cycle. The functional relevance of

SUMO modification of proteins is still poorly understood. Studies of specific SUMO-modified proteins have revealed possible roles in the regulation of protein-protein interaction (Pfander et al., 2005), transcription (Desterro et al., 1998), protein localization (Matunis et al., 1996), and more recently heat shock (Golebiowski et al., 2009). However, it has been difficult to generalize these examples to draw conclusions about target recognition, selectivity, and the mechanisms connecting SUMO modification to downstream phenotypes. Therefore, there has been much interest in the development of tools to globally characterize SUMOylation events using biochemical methods. These efforts have provided valuable clues as to the significance of SUMO modification (Desterro et al., 1998; Golebiowski et al., 2009; Gostissa et al., 1999; Ulrich, 2009). However, because of the highly dynamic nature of SUMO modification, it has remained difficult to globally assess the temporal aspects of SUMOylation in the regulation of basic biological processes.

Surprisingly, very few small molecule tools have been developed for exploring this class of protease. Currently, only inhibitors based on full-length or truncated forms of SUMO containing a reactive functional group at the C-terminal glycine residue have been described. Covalent inhibitors containing vinyl sulfone (VS) or mechanistically similar vinyl methyl ester (VME) reactive groups have been reported (Borodovsky et al., 2005; Hemelaar et al., 2004). The commercially available full-length SUMO vinyl sulfone inhibitor has also been developed into an active site probe by addition of an HA tag at the N terminus to allow detection by western blotting (Wilkinson et al., 2005). In addition, a biotinylated vinyl sulfone-based inhibitor containing the final five amino acids of the C terminus of SUMO was shown to label at least one protein in cell lysates in a dose-dependent manner (Borodovsky et al., 2005). Labeling of this protein could also be competed away by addition of full-length SUMO. However, the identity of the target has never been confirmed.

Recently, we screened a library of cysteine protease inhibitors in lysates of the human parasite pathogen *Plasmodium falciparum* to identify compounds that blocked endopeptidase processing of recombinant ProSUMO (see Ponder et al., 2011 [this issue of *Chemistry & Biology*]). This previously described library (Arastu-Kapur et al., 2008) contained 508 inhibitors

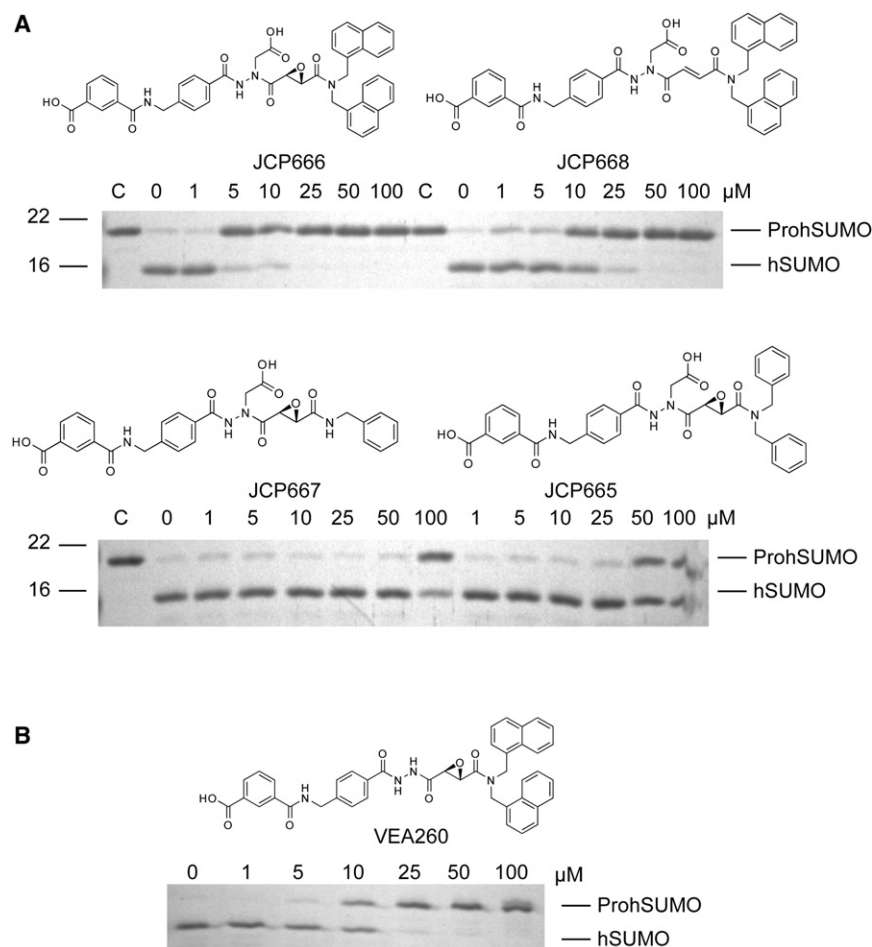


**Figure 1. Activity of Initial Lead Compounds against hSEN1P1 Using the ProSUMO Processing Assay**

(A) Purified recombinant  $\Delta$ NhSEN1P1 (100 nM) was pretreated with JCP665, JCP666, JCP667, or JCP668 (0–100  $\mu$ M) for 30 min at room temperature followed by addition of ProhSUMO1 substrate. Cleavage of ProhSUMO1 was assessed by SDS-PAGE and visualized by Gelcode Blue protein stain reagent. ProhSUMO1 alone was included as a control in the lanes labeled (C).

(B) Activity of the first-generation analog of JCP666 lacking the aza-aspartic acid side chain on the azide nitrogen. VEA260 was measured using the same assay conditions outlined in (A).

ural peptide backbone (Figure 1A). We also identified three structurally related analogs of JCP666 that differed either in the type of reactive electrophile or in the size of the aromatic groups linked to the reactive electrophile. Structure activity relationship (SAR) studies of these four compounds against the parasite SENP1 indicated that conversion of the aza-epoxide (JCP666) to an aza-acrylamide (JCP668) resulted in a modest loss of potency. Furthermore, reduction in the size of the aromatic groups attached at one end of the epoxide moiety resulted in a more dramatic loss in potency. Since these compounds were not initially tested against the human SENP proteases, we initially set out to evaluate their activity against the catalytic domain of recombinantly expressed human SENP1. To assess activity, we used a ProSUMO processing assay that makes use of a recombinantly expressed hSUMO containing the full proSUMO sequence with the addition of a C-terminal His6x tag. Since removal of the pro-region and the His6x tag results in a significant shift in the molecular weight of the SUMO protein, it is possible to monitor cleavage by simple SDS-PAGE analysis (Figure 1A). As expected based on the homology of parasite and human SENP1 proteases, the three original aza-epoxides from the library screen showed virtually identical SAR profiles as those observed for PfSEN1P1. We recently found that the aza-aspartic acid epoxides containing the bulky di-naphthyl amide were found to be somewhat susceptible to ring opening of the epoxide in aqueous media (Ponder et al., 2011 [this issue of *Chemistry & Biology*]). We found that removal of the aspartic acid side chain to generate VEA260 resulted in a more stable compound that also retained full activity against hSEN1P1 (Figure 1B). Importantly, this compound showed comparable potency to the original JCP666 lead. We therefore proceeded with this general scaffold for the rest of our SAR studies of the aza-epoxide containing compounds.

with a variety of reactive electrophiles all designed to irreversibly inhibit proteases. The screen yielded one lead compound JCP666, that contained a reactive aza-epoxide electrophile linked to an extended, nonnatural peptide backbone structure that effectively blocked PfSEN1P1 activity. In this study, we describe the application and further development of this lead series of compounds to human SENPs. Furthermore, we describe the design, synthesis, and optimization of a second class of inhibitor that contains the acyloxymethyl ketone (AOMK) reactive group. The data from these two compound classes provided an initial SAR series that resulted in the identification of compounds that covalently inhibit the catalytic domain of multiple hSENPs. Our best lead compounds were also converted to labeled analogs and used as activity-based probes. These new reagents will likely have value in the further study of SENP function.

## RESULTS AND DISCUSSION

### Evaluation of aza-epoxides as Inhibitors of Human SENPs

Our recent screen for inhibitors of the primary SENP from *Plasmodium falciparum* identified one lead compound, JCP666, that contains a reactive aza-epoxide electrophile with a nonnat-

nally expressed human SENP1. To assess activity, we used a ProSUMO processing assay that makes use of a recombinantly expressed hSUMO containing the full proSUMO sequence with the addition of a C-terminal His6x tag. Since removal of the pro-region and the His6x tag results in a significant shift in the molecular weight of the SUMO protein, it is possible to monitor cleavage by simple SDS-PAGE analysis (Figure 1A). As expected based on the homology of parasite and human SENP1 proteases, the three original aza-epoxides from the library screen showed virtually identical SAR profiles as those observed for PfSEN1P1. We recently found that the aza-aspartic acid epoxides containing the bulky di-naphthyl amide were found to be somewhat susceptible to ring opening of the epoxide in aqueous media (Ponder et al., 2011 [this issue of *Chemistry & Biology*]). We found that removal of the aspartic acid side chain to generate VEA260 resulted in a more stable compound that also retained full activity against hSEN1P1 (Figure 1B). Importantly, this compound showed comparable potency to the original JCP666 lead. We therefore proceeded with this general scaffold for the rest of our SAR studies of the aza-epoxide containing compounds.

### Design and Synthesis of Epoxide Inhibitor Library

Because our initial small SAR study confirmed that large aromatic groups were required at one end of the epoxide electrophile,

we decide to focus our efforts on the peptide-like region of our lead compound VEA260. Although VEA260 does not contain standard amino acids in the main backbone, it contains two amide linkages that are likely to represent the classical P2 and P3 residues of peptide-based inhibitors. We therefore started out synthesizing a library of compounds in which either the P2 or P3 residue was replaced by a series of natural and nonnatural amino acids (Figure 2A). In total, we synthesized six P2 compounds and nine P3 compounds.

In order to facilitate synthesis of these compounds, we developed a solid-phase synthesis method in which the terminal isophthalic acid was linked to the resin using an amide linkage. The diverse amino acids were then attached as methyl esters and subsequently converted to the hydrazide followed by coupling of the epoxide electrophile (Figure 2B). Use of a PEG-based Rink resin permitted the use of methanol as the solvent for the hydrazide formation but ultimately led to a terminal amide after cleavage from the resin. Attempts to transfer this methodology to a PEG-based Wang resin were unsuccessful as treatment with hydrazine appeared to cleave the dipeptide from the resin. Thus, unlike the original VEA260 compound that contains a terminal carboxylic acid, all of the resulting library compounds contain a terminal amide. We also synthesized VEA389, which is the amide analog of VEA260 in order to determine the impact of conversion of the terminal acid group to an amide. The P3 library was synthesized in a similar manner, except that standard Fmoc-protected amino acids were attached to the Rink resin followed by coupling of monomethyl terephthalic acid and conversion to the azide.

### Design and Synthesis of AOMK Inhibitor Library

Peptide AOMKs have been successfully used as covalent, irreversible probes of multiple classes of cysteine protease (Berger et al., 2006; Bromme et al., 1994; Sexton et al., 2007). Furthermore, these compounds can be readily synthesized using solid-phase synthesis methods (Kato et al., 2005). Therefore, we decided to explore the use of the AOMK as an alternative electrophile for hSENP inhibitors. For our first library, we retained the overall structure of VEA260 and JCP666 but used a glycine or aspartic acid residue in the P1 AOMK position (Figure 3A). Furthermore, because we determined that bulky aromatic residues near the reactive electrophile enhanced binding, we synthesized compounds that contained AOMKs with O-acyl groups increasing in size. Finally, we included a nitro-phenol in the P3 position to replace the isophthalic acid to explore diversity in this position. We were able to synthesize this library of seven compounds using standard solid-phase synthesis methods already reported for the other classes of AOMK-based inhibitors and activity-based probes (Kato et al., 2005). In addition, we also generated a small library of peptide AOMKs based on natural amino acid sequences. Data from positional scanning substrate libraries suggest that hSENPs 1–5 show a preference for the QTGG sequence which corresponds to the conserved cleavage site on all three SUMOs; however, hSENPs 6 and 7 prefer the LRGG sequence common to ubiquitin and Nedd8 (Drag et al., 2008). Therefore we synthesized both of these sequences with various truncations of the native SUMO sequence (Figure 3B). For all of these natural peptide AOMKs, we used a large O-acyl-anthracene group in the hopes of improving potency.

These peptide AOMKs are particularly interesting compounds because they are mimetics of the peptide vinyl sulfone inhibitors previously reported as hSENP inhibitors (Borodovsky et al., 2005). Therefore, they allow direct comparison of the utility of the AOMK and VS reactive groups for this class of proteases.

### Screening of Compound Libraries against Recombinant hSENPs

We initially screened all of the newly synthesized inhibitors for activity against a number of human SENPs. Humans have six SENPs that are responsible for both iso- and endo-peptidase processing of four human SUMO proteins. While the exact biological roles of each SENP are not well defined, each has different levels of iso- and endo-peptidase activity as well as different specificities for the various hSUMOs (Mikolajczyk et al., 2007). Because the original Pro-SUMO processing assay is rather tedious and not suitable for use with large numbers of compounds, we decided to screen our libraries using fluorogenic substrates that could be analyzed using a simple plate reader assay. We used the coumarin-based substrates, Ac-QTGG-AFC for hSENPs 1, 2, and 5 and Ac-LRGG-AFC for hSENPs 6 and 7 (Drag et al., 2008). Human SENP3 was not screened in this assay due to low solubility and poor activity of the recombinant enzyme. Because we had a large number of initial compounds and needed to perform the assay in triplicate, we initially used a single, high concentration of each compound to preincubate with the enzyme for 1 hr followed by measurement of the residual activity using the reporter substrates. From these data, we could determine relative inhibitor potency by comparing percentage of inhibition of the target protease for each of the library compounds (see Figures S1 and S2 available online). The results of the screens for both the aza-epoxide and AOMK libraries against all five hSENPs could then be plotted as a heat map that allows easy comparison of the complete data set (Figure 4).

From the SAR data set, we observed several general trends that could be used in our efforts to identify the most optimal inhibitors for conversion to ABPs. First, we found that conversion of the terminal acid of VEA260 to an amide resulted in a significant loss in overall activity of the compounds (compare VEA260 to VEA389). Since all of our aza-epoxides were synthesized using the solid-phase method that resulted in the generation of a terminal amide, they were all either equal or less potent than the original lead compounds. Interestingly, VEA422, which contains a P3 aspartic acid showed similar potency to the parent VEA260, suggesting that a negative charge in this general region may be important for target binding. We also found that several of the most potent aza-epoxides contained a threonine residue in either the P2 or P3 positions. This suggests that there may be key binding interaction with the enzyme at the S3 pocket that normally binds the P3 threonine of the native SUMO substrate.

From the AOMK library A, we determined that potency of the compounds dramatically increased as the ring size of the O-acyl group was increased from phenyl to naphthyl to anthracene. This finding is consistent with the observed trend in the aza-epoxides and suggests that significant contacts are required in what is likely to be the side of the active site that accommodates the prime-side sequence of the substrate. This

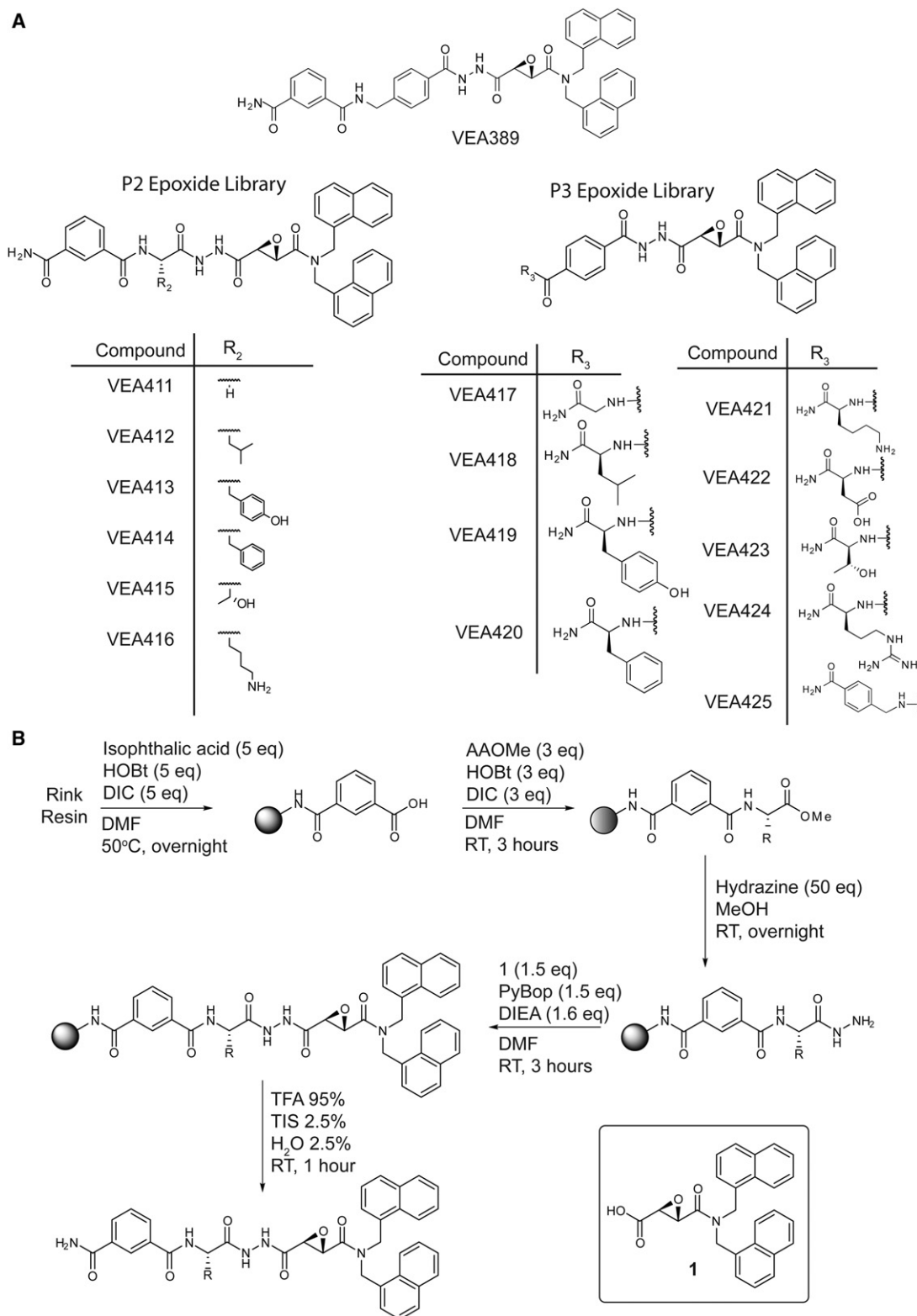


**Figure 2. Generation of a Library of Peptide Aza-Epoxides Based on VEA260**

(A) Structures of the P2 and P3 libraries along with the structure of VEA389, the direct analog of VEA260 containing a terminal amide in place of the carboxylic acid.

(B) Scheme for synthesis of the P2 library. The epoxide electrophile building block (1) is shown.

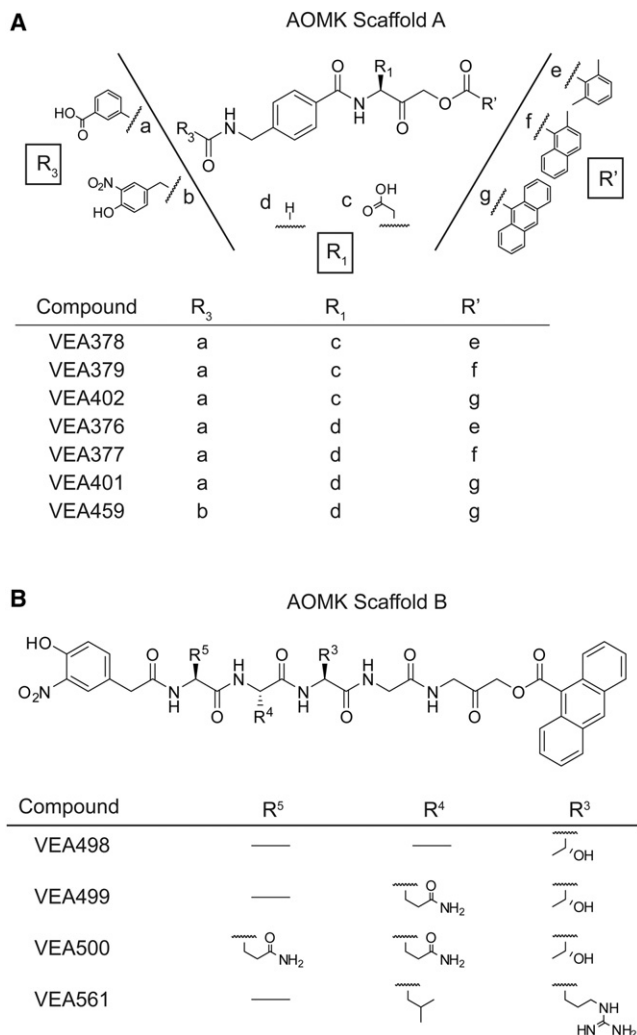


**Figure 3. Structures of Acyloxymethyl Ketone (AOMK) Inhibitor Libraries**

(A) Structures of compounds from scaffold A containing the original P2 element of VEA260 and variable P1 and P3 elements. Inhibitors were synthesized as described in the [Supplemental Experimental Procedures](#). Scaffold A was used to assess aryl group size, P1 aspartic acid versus glycine, and importance of capping group.

(B) Structures of scaffold B AOMKs based on the natural amino acid sequence found in SUMO and Ubiquitin.

could be explained by the fact that SENPs are capable of processing isopeptides that contain a large protein substrate in this prime-side region. In addition, the SAR data confirmed the lack of preference for a P1 aspartic acid residue found in the original JCP666. In fact, the P1 glycine AOMKs were more potent than the P1 aspartic acid AOMKs. This result is not surprising given the fact that SENPs bind to substrates with a P1 glycine. Finally, the results from the natural peptide AOMKs in library B demonstrated the need for an extended peptide to facilitate binding in the SENP active site. Specifically, we found that the tetrapeptide (VEA499) and pentapeptide (VEA500) inhibitors based on the natural sequence of hSUMO1 were substantially more potent than the tripeptide (VEA498) equivalent. In addition,

VEA561 which contains the sequence of ubiquitin, was most potent toward hSENP6 and hSENP7, consistent with the published specificity of these proteases ([Drag et al., 2008](#)). Overall, our results suggested that the extended peptide AOMKs based on the natural SUMO sequence were most potent followed closely by the AOMKs containing parts of the JCP666 scaffold.

To further characterize and more accurately rank the best inhibitors identified in the fixed concentration screen, we selected the most active compounds from the P2/P3 aza-epoxide and AOMK libraries and determined IC<sub>50</sub> values for hSENP1, 2, 6, and 7 using the fluorogenic substrate assay ([Table 1](#); [Figure S3](#)). Due to the low activity and limited solubility of hSENP5, IC<sub>50</sub> values could not accurately be determined. The results revealed that VEA260 was the most potent aza-epoxide inhibitor for hSENP1, 2, and 7 and none of the aza-epoxides were able to inhibit hSENP6. The AOMK based on the ubiquitin sequence (VEA561), however, was the most potent overall inhibitor against both hSENP6 and hSENP7, while the AOMK with the QTGG specificity sequence (VEA499) was most potent overall for hSENP1 and hSENP2.

We also wanted to test the potential for cross-reactivity of both the epoxide and AOMK classes of inhibitors against related proteases. Specifically, the AOMK inhibitor VEA561 has the sequence LRGG-AOMK which matches the sequence found on the C terminus of Ubiquitin and NEDD8. We therefore tested VEA260, VEA499 (QTGG) and VEA561 (LRGG) against the purified human DUB UCHL3 and human SENP8 (a deNEDDylase) to determine if the compounds were active against these off-targets (see [Figure S4](#)). Interestingly, VEA260 showed virtually no activity against either enzyme and the two AOMK probes show only activity against hSENP8. We also confirmed that VEA401 did not block labeling of DUBs in HEK293 cell lysates by the HA-Ubvme probe ([Figure S4](#)), again suggesting that the best SENP inhibitors do not have significant activity against DUBs.

Although the AOMK-based inhibitors were generally active as SENP inhibitors, we were concerned that these compounds may not gain access to the SENPs due to overall low cell permeability. We therefore tested our best AOMK compound with the least peptide character, VEA401 in intact cells. Specifically, we treated intact HeLa cells with VEA401 for 3 hr and then labeled endogenous SENPs in lysates using a full-length SUMO2 probe (HA-SUMO2-VME) ([Figure S5](#)). These results suggested that the compound failed to gain sufficient access to either hSENP1 or hSENP6 to block labeling by the HA-SUMO2-VME probe. In addition, we were not able to find conditions in which we could treat cell lysates with VEA401 and block labeling of endogenous SENP1 or SENP6 by the HA-SUMO2-VME probe. This is likely due to the low levels of stable and active SENPs in lysates and the overall slow binding of the AOMK compounds compared with binding full-length SUMO probes. We therefore feel that the AOMK probes will require further development in order to be made sufficiently cell permeable to allow complete inhibition of SENP targets.

#### Design and Synthesis of ABPs

One of primary goals of this study was to develop new reagents that could be used as activity-based probes of hSENP activity. We therefore decided to synthesize a series of biotin and Cy5

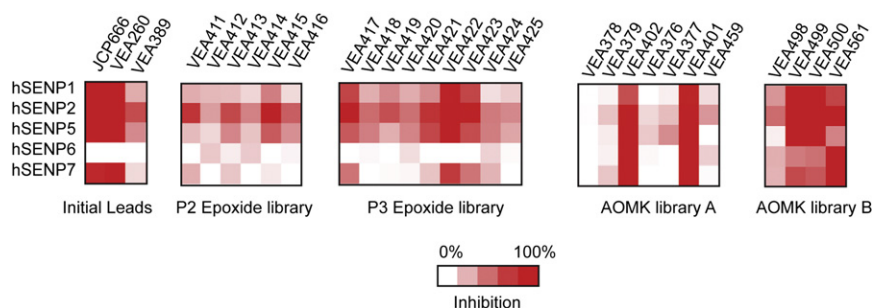


**Figure 4. Activity of Aza-Epoxyde and AOMK Inhibitors against Recombinant hSENP Proteases**

Recombinant purified  $\Delta$ NhSENPs1, 2, 5, 6, and 7 were incubated with 50  $\mu$ M inhibitors. After addition of either Ac-QTGG-AFC for  $\Delta$ NhSENPs 1, 2, and 5 or Ac-LRGG-AFC for  $\Delta$ NhSENPs 6 and 7, the AFC production at 405 nm/510 nm for 10–60 min was measured using a fluorescence plate reader. Activity relative to the DMSO-treated control was determined and average values from triplicate runs are shown as a heat map where red indicates 100% inhibition and white indicates 0% inhibition. See also Figures S1 and S2.

fluorescent-labeled probes based on the most potent AOMK and aza-epoxyde compounds identified in our SAR screen (Figure 5A). In addition, we synthesized a previously reported biotin-labeled pentapeptide vinyl sulfone (Bio-EQTGG-VS) and a vinyl methyl ester (Bio-QQTGG-VME) for comparison with our newly identified compounds. Before using these compounds as probes, we first tested them for potency against all the hSENPs in our fluorogenic substrate assay (Figure 5B; Figure S6). As expected, the AOMK probe VEA505 was most potent. The aza-epoxyde probe VEA355 also showed reasonable potency against primarily hSENP1 and 2. Notably, the VS and VME probes showed almost no inhibitory activity even at the highest concentration of the assay.

We next tested the ability of the probes to label the recombinant hSENPs. We added each of the probes to recombinant hSENP1 and 2 and monitored labeling by analysis by SDS-PAGE followed by blotting for biotin or scanning for fluorescence (Figure 5C). In addition, we pretreated the recombinant enzymes with the inhibitor versions of the probes as well as with the general cysteine alkylating agent *N*-ethylmaleimide (NEM) to block the active site. These results indicated that both the aza-epoxyde and AOMK probes efficiently labeled both hSENPs. To confirm that labeling was due to modification of the active site cysteine, we also labeled a mutant hSENP2 in which the active site cysteine was converted to serine (hSENP2 C548S, Tables S1 and S2). As expected, the AOMK probe VEA505 no longer was able to label the mutant protease, while aza-epoxyde probe VEA355 showed a faint labeling suggesting that it may be nonspecifically modifying noncatalytic cysteine residues. The Cy5-labeled version of VEA355 also showed what appeared to be a doublet of bands, again suggesting that it might be modifying multiple cysteine residues resulting in different migration in the gel. Interestingly, neither the previously reported vinyl sulfone nor the vinyl methyl ester probes labeled either of the hSENP proteases, consistent with their inability to inhibit the recombinant proteases in the substrate assay. We also monitored the kinetics of enzyme labeling over a period of 30 min to 7 hr (Figure 5D). These results demonstrated that labeling by the AOMK-based probe VEA505 was relatively fast with labeling detectable at the first time point for hSENP2. However, by comparison the aza-epoxyde probe showed slower labeling of the enzyme. Interestingly, we also observed a slight upward shift in mobility over time when labeling with Cy5-VEA355 consistent with labeling multiple cysteine residues leading to a change in migration in the gel. Based on these findings, it seemed that

the AOMK probe was more suited for use as an ABP since it reacted faster and showed less nonspecific labeling compared with the aza-epoxyde probe.

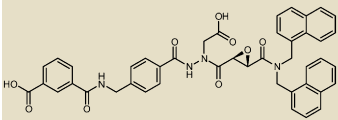
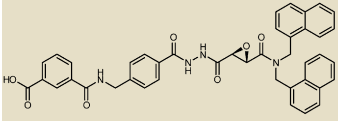
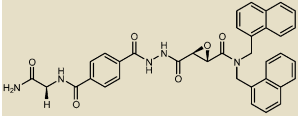
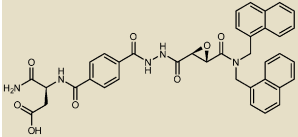
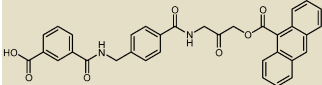
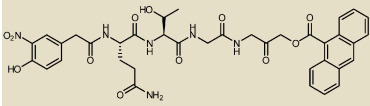
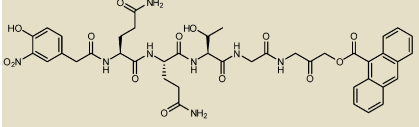
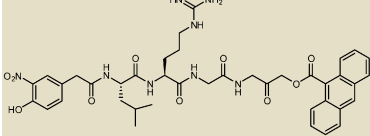
#### Labeling of hSENP1 in Complex Proteomes

As a final test to determine the selectivity of our ABPs for hSENP proteases, we evaluated their ability to label a target hSENP in a complex proteome. For this study, we added the recombinant hSENP1 to total lysates from HEK293 cells. We then labeled the lysates with a serial dilution of biotinylated or fluorescent aza-epoxyde and AOMK probes (Figure 6A). These results demonstrated that the aza-epoxyde probes were highly reactive and produced high background labeling even at the lowest probe concentration tested. Furthermore, we were not able to detect any labeling of the hSENP for either the fluorescent or biotin-labeled aza-epoxyde probes. The AOMK, on the other hand, produced clean labeling of the hSENP with only moderate background observed for high concentrations of the biotin probe. Addition of the Cy5 probe produced clean labeling of the hSENP that could be detected with less than 1  $\mu$ M probe concentration. We found that the biotin-VEA505 was also able to label hSENP1 at similar concentrations of the probe relative to the Cy5 version of the probe. We also tested the activity of the biotin and Cy5 probes in the ProSUMO processing assay (Figure S7). Interestingly, these data suggest that the Cy5 version of the probe was able to block substrate processing more effectively than the biotin version. Finally, for comparison, we performed the same labeling experiment using the full-length SUMO probes containing a C-terminal vinyl sulfone or vinyl methyl ester and an HA tag (Figure 6B). As expected these probes produced clean labeling of the target SENP with the VME probe showing similar selectivity and sensitivity as the Cy5-VEA505. As a final test of sensitivity, we used the biotin and Cy5 versions of VEA505 to label recombinant hSENP1 that has been added to cell extracts at a range of concentrations relative to the background proteome (Figure S8). These data confirm that both probes have similar sensitivity and can label as little as 100 nM of the enzyme in a complex proteome. These results suggest that probes based on the peptide AOMKs are valuable new ABPs that can be as efficient and selective as the full-length protein-based probes.

#### SIGNIFICANCE

**The process of protein SUMOylation and deSUMOylation is dynamic. Therefore, the SENP proteases involved in the**

**Table 1. IC<sub>50</sub> Values of Most Potent Aza-Epoxy and AOMK Inhibitors**

	IC <sub>50</sub> Values (μM)			
	hSENP1	hSENP2	hSENP6	hSENP7
 JCP-666	13.8 ± 1.0	7.0 ± 0.4	>100	>70
 VEA-260	7.1 ± 0.6	3.7 ± 0.2	>100	36.5 ± 4.7
 VEA-417	32.5 ± 2.8	13.1 ± 1.3	>100	>70
 VEA-422	22.4 ± 2.1	10.4 ± 0.7	>100	>70
 VEA-401	23.1 ± 1.6	13.4 ± 1.2	>40	>20
 VEA-499	3.6 ± 0.3	0.25 ± 0.03	>60	>100
 VEA-500	>20	0.86 ± 0.1	>40	>100
 VEA-561	>25	5.7 ± 1.6	4.2 ± 0.6	4.3 ± 0.7

Recombinant purified ΔNhsENPs 1, 2, 6, and 7 were incubated with inhibitors (195 nM to 100 μM). After addition of either Ac-QTGG-AFC for ΔNhsENPs 1 and 2 or Ac-LRGG-AFC for ΔNhsENPs 6 and 7, AFC production was measured in triplicate using a fluorescence plate reader at 405 nm/510 nm for 10–60 min. Activity relative to the DMSO-treated control was determined and IC<sub>50</sub> values calculated using GraFit 6 as described in [Experimental Procedures](#). See also [Figure S3](#).

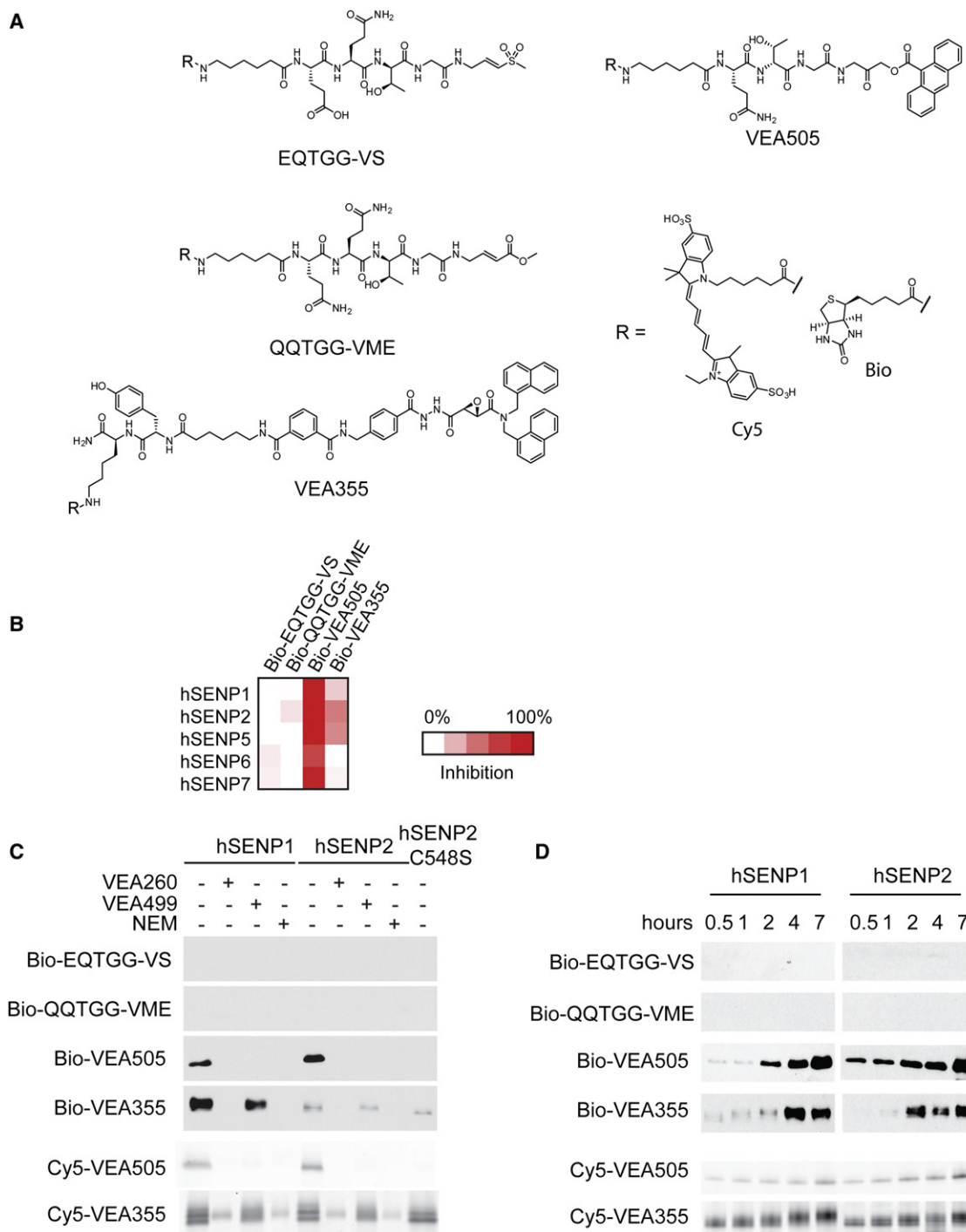


**Figure 5. Development of Activity-Based Probes for hSENPs Based on the Most Potent AOMK and Aza-Epoxy Inhibitors**

(A) Structures of the AOMK and aza-epoxide probe scaffolds along with the peptide vinyl sulfone and vinyl methyl ester probes. For each probe, the R group was either a biotin tag or Cy5 fluorescent tag as indicated in the name of the compound.

(B) Heat maps showing the activity of all the biotin versions of the probes (50  $\mu$ M) against the recombinant hSENPs.

(C) Labeling of recombinant hSENP1 and hSENP2.  $\Delta$ NhSENP2.  $\Delta$ NhSENP2 C548S (0.5  $\mu$ M) were labeled with probe (1  $\mu$ M) after pretreatment with either with vehicle (-) or with VEA260 (epoxide inhibitor, 50  $\mu$ M), VEA499 (AOMK inhibitor, 50  $\mu$ M), or N-ethylmaleimide (NEM, 20 mM) as indicated. Proteins were resolved by SDS-PAGE and labeling visualized by biotin affinity blotting using horseradish peroxidase-conjugated streptavidin for the biotinylated probes. Cy5 probe labeling was resolved by SDS-PAGE and visualized using a flatbed scanner.

(D) Purified recombinant  $\Delta$ NhSENPs 1 and 2 (0.5  $\mu$ M) were treated with probe (1  $\mu$ M) for increasing time (30 min to 7 hr). Samples were visualized as described above. See also Figure S4.

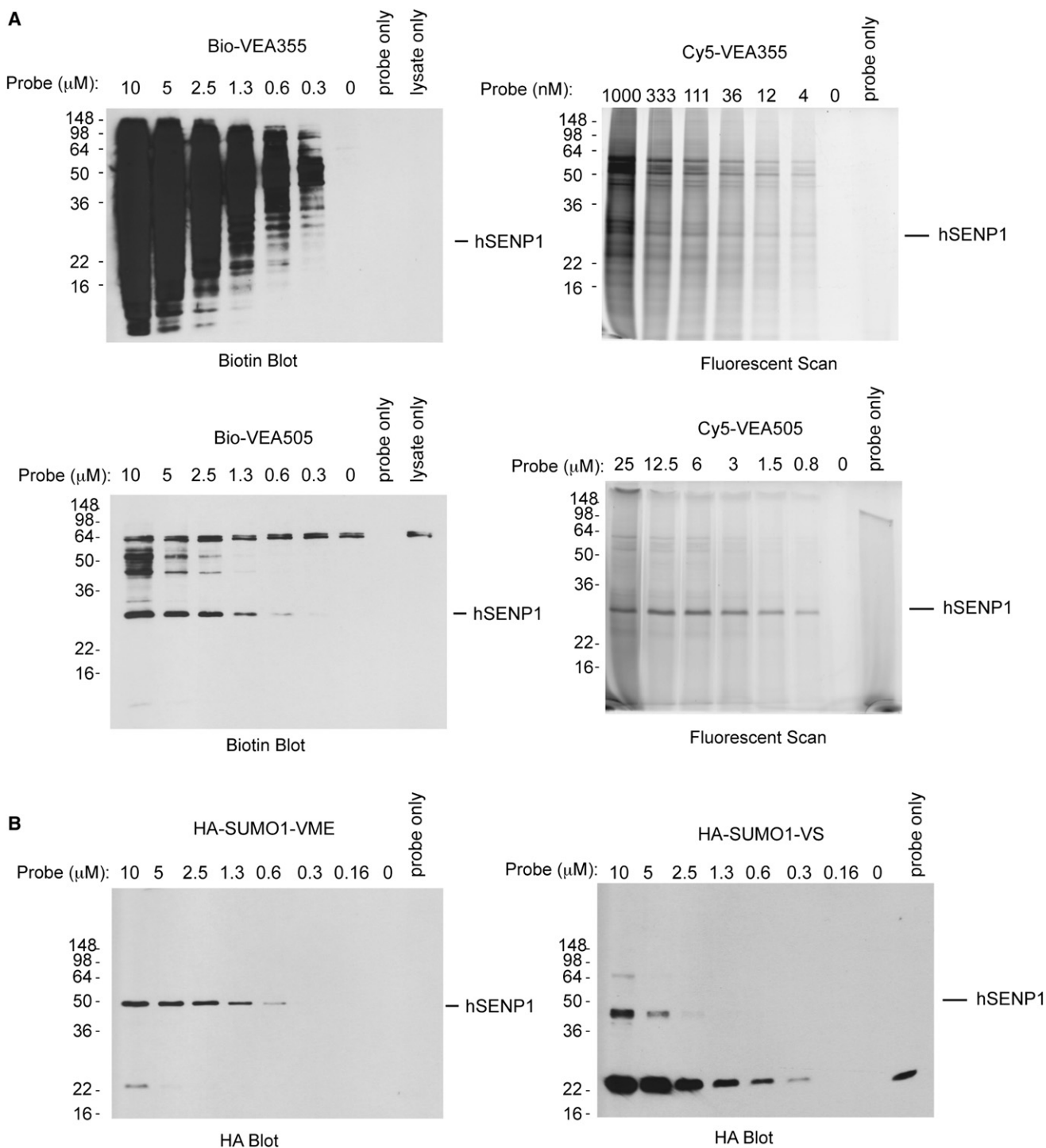


**Figure 6. Labeling of Recombinant hSENP1 in Complex Proteomes**

(A) Recombinant  $\Delta\text{NhSENP1}$  was spiked into hypotonic HEK293 cell lysates as 0.1% of the total protein mixture (25 ng  $\Delta\text{NhSENP1}$  in 25  $\mu\text{g}$  of lysate). The spiked lysate was treated with decreasing concentrations of probes (Bio-VEA355, Bio-VEA505, Cy5-VEA355, and Cy5-VEA505) for 1 hr at 37°C. Proteins were resolved by SDS-PAGE and visualized as described above.

(B) Recombinant  $\Delta\text{NhSENP1}$  spiked into hypotonic HEK293 cell lysates was treated with decreasing concentrations of apparent active full-length SUMO VS and VME probes. Proteins were resolved by SDS-PAGE and visualized by western blot using an anti-HA antibody.

production of SUMO precursor and deconjugation of SUMO from substrates are fundamental for a number of biological processes regulated by SUMOylation. Unfortunately, there are no optimal methods to temporally regulate the activity of SENPs. Current reagents for studying SENP activity require a full-length protein with an electrophile for covalent modification of the proteases. In this study, we present two new small molecule scaffolds that can be used as inhibitors and activity-based probes of the hSENPs. Our results suggest that peptide aza-epoxides are relatively efficient inhibitors of various SENPs, but these reagents show high nonspecific labeling properties when used in complex proteomes. Peptide AOMKs containing a large aromatic O-acyl group, on the other hand, are covalent inhibitors that also function as highly selective probes of SENP activity. While further work is required to increase the potency of these compounds, we believe that they are an important new class of reagents for the study of SENP function.

## EXPERIMENTAL PROCEDURES

### Synthetic Protocols

See Supplemental Experimental Procedures.

### Cloning and Expression of hSENP1, 2, 5, 6, and 7

All final constructs and primers are summarized in Tables S1 and S2. The catalytic mutant of hSENP2 (C548S) was generated by PCR-SOE (primers #1–4) and ligated into the pET28a vector for expression. All constructs were expressed in BL21(DE3) *Escherichia coli* (OD<sub>600</sub> = 0.6; 0.1 mM IPTG) for 3 hr at 30°C, lysed in 50 mM HEPES (pH 7.4), 100 mM NaCl, 5% glycerol, 5% sucrose, immobilized on Ni<sup>2+</sup>-NTA agarose (QIAGEN), and eluted with stepwise fractions of lysis buffer (50 mM HEPES [pH 7.4], 100 mM NaCl, 5% glycerol, 5% sucrose) supplemented with 20–200 mM imidazole. The hSENPs were prepared as previously described (Mikolajczyk et al., 2007).

### ProSUMO Cleavage Assays

SUMO-pro cleavage assays were performed as previously described (Mikolajczyk et al., 2007). In brief, 100 nM hSENP1 in reaction buffer (50 mM Tris [pH 7.4], 5 mM NaCl, 5 mM DTT) was pretreated with inhibitor (JCP665-8) for 30 min at 37°C and then allowed to cleave SUMO-pro protein for 1 hr at 37°C. Proteins were separated by SDS-PAGE and visualized by Gelcode Blue protein stain reagent (Pierce).

### Fluorogenic Substrate Assay

The fluorogenic substrate library screen was performed as described previously (Drag et al., 2008). In brief, hSENP1 (final concentration 2 μM) in low salt Tris buffer (50 mM Tris [pH 8.0], 20 mM NaCl, 10 mM DTT) was preincubated for 1 hr at 37°C with inhibitor (50 μM final concentration) followed by addition of substrate (100 nM). Fluorophore release (AFC) was monitored for 30 min at 37°C with an excitation of 405 nm and emission at 510 nm. Rates of cleavage were determined as the slope of the linear line representing RFU/min. The DMSO-treated sample was set as 100% activity, and the activity of the other samples was determined relative to this value. All values are the average of independent triplicates.

### IC<sub>50</sub> Determinations

IC<sub>50</sub>'s for the inhibitors were determined by serial dilution of the compounds in the fluorogenic assay described above. The assay was repeated three or four times per compound and the IC<sub>50</sub> determined using Graphfit software.

### Time Course of Labeling of Recombinant hSENP1 and 2 with Activity-Based Probes

Recombinant ΔhSENP1 or 2 was diluted to 0.5 μM in reaction buffer (50 mM Tris [pH 7.4], 20 mM NaCl, 5 mM DTT) and treated with probe (1 μM final

concentration of Bio-EQTGG-VS, Bio-QQTGG-VME, Bio-VEA505, Bio-VEA355, Cy5-VEA505, Cy5-VEA355) for varying time (30 min to 7 hr) at 37°C. Proteins were separated by SDS-PAGE. Fluorescent gels were scanned using a Typhoon 9400 flatbed laser scanner (GE-Healthcare). All other gels were visualized by biotin affinity blotting using horseradish peroxidase-conjugated streptavidin.

### Labeling and Competition for Recombinant hSENP1 and 2 Activity with Activity-Based Probes

Recombinant ΔhSENP1 or 2 or ΔhSENP2 C548S was diluted to 0.5 μM in reaction buffer (50 mM Tris [pH 7.4], 20 mM NaCl, 5 mM DTT) and treated with either DMSO, VEA260, VEA499 (both 50 μM final concentration) or *N*-ethylmaleimide (20 mM final concentration) for 1 hr at 37°C. Labeling was carried out with 1 μM final probe concentration (Bio-EQTGG-VS, Bio-QQTGG-VME, Bio-VEA505, Bio-VEA355, Cy5-VEA505, Cy5-VEA355) for 1 hr at 37°C. Proteins were separated by SDS-PAGE. Fluorescent gels were scanned using a Typhoon 9400 flatbed laser scanner (GE-Healthcare). All other gels were visualized by biotin affinity blotting using horseradish peroxidase-conjugated streptavidin.

### Labeling of Recombinant hSENP1 Spiked into HEK293 Cell Lysates

Recombinant ΔhSENP1 (25 ng) was added to HEK293 cell lysates (25 μg) in reaction buffer (50 mM Tris [pH 7.4], 20 mM NaCl, 5 mM DTT) and treated with serial dilution of probe (Bio-VEA505, Bio-VEA355, Cy5-VEA505, Cy5-VEA355, HA-SUMO1-VME, HA-SUMO1-VS) for 1 hr at 37°C. Proteins were separated by SDS-PAGE. Fluorescent gels were scanned using a Typhoon 9400 flatbed laser scanner (GE-Healthcare). Biotinylated probes were visualized by biotin affinity blotting using horseradish peroxidase-conjugated streptavidin and full-length SUMO probes were visualized using an anti-HA antibody.

### Lysate Preparation

Lysates of HEK293 cells were prepared from cells grown as a 90% confluent monolayer. The cells were washed with PBS before being scraped and transferred to an Eppendorf tube. The cells were spun down at 2000 rpm for 4 min and the PBS was removed. An equivalent volume of hypotonic lysis buffer (20 mM Tris [pH 7.4], 5 mM NaCl, and 5 mM DTT) was added to the pellet. The mixture was allowed to sit on ice for 10 min before mechanical lysis through a 26.5 gauge needle. The mixture was spun down at maximum speed for 30 min at 4°C. The supernatant was transferred and quantified to be 8 mg/ml.

## SUPPLEMENTAL INFORMATION

Supplemental Information includes Supplemental Experimental Procedures, Supplemental Compound Characterization, eight figures, and two tables and can be found with this article online at doi:10.1016/j.chembiol.2011.05.008.

## ACKNOWLEDGMENTS

We thank P. Bowyer and A. Shen for creative discussion and L. Edgington, A. Puri, and J. Valderramos for outstanding technical assistance. This work was supported by NIH grants R01 EB005011, R01 AI 078947, and a New Investigator in Pathogenesis Award from Burroughs Wellcome Fund (to M.B.).

Received: December 7, 2010

Revised: May 17, 2011

Accepted: May 20, 2011

Published: June 23, 2011

## REFERENCES

- Arastu-Kapur, S., Ponder, E.L., Fonovic, U.P., Yeoh, S., Yuan, F., Fonovic, M., Grainger, M., Phillips, C.I., Powers, J.C., and Bogoy, M. (2008). Identification of proteases that regulate erythrocyte rupture by the malaria parasite *Plasmodium falciparum*. *Nat. Chem. Biol.* 4, 203–213.
- Berger, A.B., Witte, M.D., Denault, J.B., Sadaghiani, A.M., Sexton, K.M., Salvesen, G.S., and Bogoy, M. (2006). Identification of early intermediates of

- caspace activation using selective inhibitors and activity-based probes. *Mol. Cell* 23, 509–521.
- Borodovsky, A., Ovaa, H., Meester, W.J., Venanzi, E.S., Bogoy, M.S., Hekking, B.G., Ploegh, H.L., Kessler, B.M., and Overkleeft, H.S. (2005). Small-molecule inhibitors and probes for ubiquitin- and ubiquitin-like-specific proteases. *ChemBioChem* 6, 287–291.
- Bromme, D., Smith, R.A., Coles, P.J., Kirschke, H., Storer, A.C., and Krantz, A. (1994). Potent inactivation of cathepsins S and L by peptidyl (acyloxy)methyl ketones. *Biol. Chem. Hoppe Seyler* 375, 343–347.
- Desterro, J.M., Rodriguez, M.S., and Hay, R.T. (1998). SUMO-1 modification of I $\kappa$ B $\alpha$  inhibits NF- $\kappa$ B activation. *Mol. Cell* 2, 233–239.
- Drag, M., and Salvesen, G.S. (2008). DeSUMOylating enzymes—SENPs. *IUBMB Life* 60, 734–742.
- Drag, M., Mikolajczyk, J., Krishnakumar, I.M., Huang, Z., and Salvesen, G.S. (2008). Activity profiling of human deSUMOylating enzymes (SENPs) with synthetic substrates suggests an unexpected specificity of two newly characterized members of the family. *Biochem. J.* 409, 461–469.
- Geiss-Friedlander, R., and Melchior, F. (2007). Concepts in sumoylation: a decade on. *Nat. Rev. Mol. Cell Biol.* 8, 947–956.
- Golebiowski, F., Matic, I., Tatham, M.H., Cole, C., Yin, Y., Nakamura, A., Cox, J., Barton, G.J., Mann, M., and Hay, R.T. (2009). System-wide changes to SUMO modifications in response to heat shock. *Sci. Signal.* 2, ra24.
- Gostissa, M., Hengstermann, A., Fogal, V., Sandy, P., Schwarz, S.E., Scheffner, M., and Del Sal, G. (1999). Activation of p53 by conjugation to the ubiquitin-like protein SUMO-1. *EMBO J.* 18, 6462–6471.
- Hemelaar, J., Borodovsky, A., Kessler, B.M., Reverter, D., Cook, J., Kolli, N., Gan-Erdene, T., Wilkinson, K.D., Gill, G., Lima, C.D., et al. (2004). Specific and covalent targeting of conjugating and deconjugating enzymes of ubiquitin-like proteins. *Mol. Cell Biol.* 24, 84–95.
- Kato, D., Boatright, K.M., Berger, A.B., Nazif, T., Blum, G., Ryan, C., Chehade, K.A., Salvesen, G.S., and Bogoy, M. (2005). Activity-based probes that target diverse cysteine protease families. *Nat. Chem. Biol.* 1, 33–38.
- Kim, J.H., and Baek, S.H. (2009). Emerging roles of desumoylating enzymes. *Biochim. Biophys. Acta* 1792, 155–162.
- Matunis, M.J., Coutavas, E., and Blobel, G. (1996). A novel ubiquitin-like modification modulates the partitioning of the Ran-GTPase-activating protein RanGAP1 between the cytosol and the nuclear pore complex. *J. Cell Biol.* 135, 1457–1470.
- Mikolajczyk, J., Drag, M., Bekes, M., Cao, J.T., Ronai, Z., and Salvesen, G.S. (2007). Small ubiquitin-related modifier (SUMO)-specific proteases: profiling the specificities and activities of human SENPs. *J. Biol. Chem.* 282, 26217–26224.
- Pfander, B., Moldovan, G.L., Sacher, M., Hoege, C., and Jentsch, S. (2005). SUMO-modified PCNA recruits Srs2 to prevent recombination during S phase. *Nature* 436, 428–433.
- Ponder, E.L., Albrow, V.E., Leader, B.A., Békés, M., Mikolajczyk, J., Fonović, U., Shen, A., Drag, M., Xiao, J., Deu, E., et al. (2011). Functional characterization of a SUMO deconjugating protease of *Plasmodium falciparum* using newly identified small molecule inhibitors. *Chem. Biol.* 18, this issue, 711–721.
- Sexton, K.B., Witte, M.D., Blum, G., and Bogoy, M. (2007). Design of cell-permeable, fluorescent activity-based probes for the lysosomal cysteine protease asparaginyl endopeptidase (AEP)/legumain. *Bioorg. Med. Chem. Lett.* 17, 649–653.
- Ulrich, H.D. (2009). Regulating post-translational modifications of the eukaryotic replication clamp PCNA. *DNA Repair (Amst.)* 8, 461–469.
- Wilkinson, K.D., Gan-Erdene, T., and Kolli, N. (2005). Derivatization of the C-terminus of ubiquitin and ubiquitin-like proteins using intein chemistry: methods and uses. *Methods Enzymol.* 399, 37–51.